Performance Enhancement of VAWT using Diffuser for Energy Extraction from Cooling Tower Exhaust Air

Enderaaj **Singh,** ***Sukanta*** **Roy, Yam** ***Ke San*** **and Law** ***Ming Chiat***

Department of Mechanical Engineering, Faculty of Science and Engineering, Curtin University Malaysia

Email: sukanta.roy@curtin.edu.my

Abstract. Renewable energy generation need to be accelerated to battle climate change and depletion of fossil fuel resources. Innovation to design wind recovery system which are efficient is vital to contribute green energy production. Many advancements in vertical axis wind turbines (VAWT) were made over the years however, it is still not as efficient as conventional turbines, and some countries does not have the luxury of strong consistent wind throughout the year. Therefore, this study focuses on extracting wind energy from unnatural sources, specifically for cooling tower exhaust air energy recovery. In this study, cycloidal diffuser with different shroud lengths was used to study the performance of a 3-bladed H-Darrieus VAWT (HDWT) with S-1046 airfoils under accelerated wind conditions in a 3-dimensional numerical study using shear stress transport k-ω turbulence model. The cycloidal diffuser with shroud length of $0.48D$ increased the HDWT power coefficient by 26.66% compared to the bare HDWT at tip speed ratio of 2.0. Aerodynamics around the energy extractor system was also discussed and this investigation has provided good understanding of the flow behaviour of the wind augmented HDWT under cooling tower exhaust air.

1. Introduction

Globally, energy usage and demand is on the rise with the growth of industrial sectors and increase in population annually. Fossil fuel remains the major energy supply, covering 83.1% of the world total energy demand in 2021 [1]. Even though fossil fuel contribution decreased below 84% only for the second time in history, carbon emissions are still high with 36.3 billion metric tonnes emissions recorded in 2021, which is a 6% rebound from the low emission year due to global pandemic in 2020 and just 1.09% lower than the record 2019 emissions [2]. This causes worsening health issues due to rising global warming. Moreover, the conventional energy resources are depleting and effort to increase alternative source of energy such as renewable energy needs to be done intensely to supply the ever-growing energy demand. Wind energy is one of the largest and fastest growing renewable energy sources with 837 GW installed as of 2021 which reduces 1.2 billion tonnes of carbon dioxide emissions annually [3]. Energy consumption is the highest in densely populated areas due to urbanisation. Vertical axis wind turbines or VAWTs with its small design, low noise level, ability to capture winds from any direction, and adaptability to turbulent conditions are more suitable to be used for harvesting wind energy in urban areas compared to the conventional horizontal axis wind turbines (HAWTs) [4]. Numerous research is being done on VAWT design and implementation to increase its power production efficiency for urban applications. There are several studies that were successful in using VAWT's for wind energy extraction in urban area by integrating its design to urban infrastructure or placing it at locations with higher wind

speeds such as on tall buildings, street light poles, and roadside barriers [4]. VAWT can be further classified into lift and drag-type turbines. An example of a drag-type VAWT is the Savonius VAWT, while Darrieus VAWT is the most used lift-type turbine [4]. H-Darrieus wind turbines (HDWTs) have received more research interests since it can extract power with a higher coefficient and operates at wider tip speed ratio compared to Savonius turbines [4]–[6]. However, HDWT has poor start-up properties. Many studies on HDWT have been done to improve its efficiency and start-up properties. The most important parameter of a HDWT is its airfoil type. Hashem and Mohamed [5] carried out a broad two-dimensional simulation study on a 3-bladed HDWT using 24 types of airfoil, consisting of symmetrical and asymmetrical airfoil shapes which resulted in the S-1046 airfoil giving highest HDWT performance. Another important parameter for a HDWT is the turbine's solidity which is the ratio based on the chord length of the blade to the number of turbine blades used. Studies on turbine solidities showed that lower solidity HDWT performed better at higher tip speed ratios (TSR) while higher solidity produce higher power coefficient at lower TSR [7]–[9]. There are other studies conducted on HDWT which includes factors such as aspect ratio, pitch angles, strut effect, and methods to increase HDWT performance using flow augmenters [6], [10], [11].

Nonetheless, many countries face the challenge of unpredictable wind conditions to efficiently harness power from natural wind especially in urban areas. Therefore, the focus of this study is to extract wind power from man-made, unnatural wind sources from the exhaust of a cooling tower as it discharges air consistently at high velocity of up to 16m/s [12]. There have been experimental study conducted by Chong et al. [13] and numerical study conducted by Tabatabaeikia et al. [14] on extracting cooling tower exhaust air to generate power using a 5-bladed lift type VAWT. From these studies, the VAWT optimum location with the use of flow augmentation method consisting of separator plates, modified plate diffuser and guide vanes managed to rotate the VAWT faster which resulted in 13% exhaust air energy being recovered. On top of that, the presence of VAWT at the cooling tower outlet also manages to reduce the cooling tower's fan motor power consumption. In another study, Berhanu et al. [15] attempted an experimental study to recover exhaust air energy from the exhaust of a composite textile mill by using a Savonius type turbine. This was done by increasing the velocity of the exhaust air by placing a drag force blocker, which managed to increase the velocity of the air approaching the turbine by 4 times. According to the study by Berhanu et al. [15], this can potentially increase the overall energy generation efficiency by 86.8%. Nimje and Gandhi [16] executed a study to extract high exhaust air energy from cement manufacturing plant's air filter duct by first numerically optimizing the depth and diameter of a single hemispherical blade based on the filter duct outlet size. Then the blades were fabricated to experimentally test a 3-bladed and 6-bladed turbine set-up which shows the 6-bladed turbine perform better, producing 35W power [16].

Flow augmenters such as deflectors, guide vanes and diffusers can improve the VAWT performance above the Betz limit as it increases oncoming wind speed and guides it to a desired angle of attack of the turbine airfoil [11]. Deflectors are best used for drag-type VAWT or Savonius VAWT to protect the returning blade from wind and guide it towards the advancing blade to increase the positive torque [17], [18]. Nevertheless, deflectors can also enhance Darrieus VAWT performance as showed in a study by Qasemi and Azadani [19] to optimize five of the flat plate deflector parameters which managed to improve the turbine performance by 16.42%, with the plate deflector angle being the most influencing parameter. Chen et al. [20] also conducted studies to maximize the HDWT performance by optimizing two flat plate deflectors using Taguchi method and modified additive method (MAM). The optimized location of the deflector increased the turbine power coefficient by 20% [20]. Diffusers are a great flow augmenter which can greatly improve Darrieus VAWT performance, especially when designed with a shroud or nozzle and a flange or brim. The diffusers with shroud and flanges create high pressure difference between the region at the upstream and downstream of the turbine. The flanges creates low pressure at the turbine's downstream region which causes the wind from the high-pressure region upstream to accelerate through the turbine which is placed in between the diffusers, increasing the turbine performance as proved in many previous studies [5], [21]–[24]. Dessoky et al. [24] and Hashem and Mohamed [5] performed CFD studies to enhance the power performance of a VAWT by using three

types of diffusers designs namely, curved-surface diffuser, flat-panel diffuser, and cycloidal diffuser. Both these studies have shown that the power augmentation by the diffuser with a cycloidal shape is higher than the curved-surface and flat-panel diffusers. In a previous study by the author [25], cycloidal diffuser and guide vanes was adopted to investigate and compare the power coefficient improvement on the HDWT between the two types of flow augmenters. The cycloidal diffuser produced better result with 23.92% higher power coefficient at TSR 2.0 than the bare HDWT.

Most of the wind augmented VAWT studies were mainly done under free stream condition [6]. The past exhaust air energy extractor literature discussed has been done by implementing some type of flow augmentation method. However, there are more types of flow augmenters such as using shrouded diffuser with flanges have not been studied under accelerated air conditions. Therefore, this study is focused on augmenting the power coefficient of a three-bladed H-Darrieus VAWT (HDWT) by placing a shrouded cycloidal diffuser with flanges around the HDWT, under the accelerated cooling tower exhaust air in a three-dimensional numerical study. Parametric design study of the diffusers' shroud length will be conducted in this study to measure the average moment coefficient and power coefficient of the HDWT with analysis of the flow behaviour around the exhaust air energy extractor system in cooling tower application.

2. Methodology

2.1. Parameters for HDWT performance measure

The HDWT for this study will be tested at different rotational speed. Therefore, the parameter, tip speed ratio (TSR) is important for this study which is known as ratio of the HDWT translation speed compared to free stream velocity, V_∞ [m/s] shown in Equation (1) with ω denoting the angular velocity of the turbine [rad/s] and radius of the turbine is denoted as R [m]. Equations (2) and (3) are used to measure the HDWT performance which are the average coefficient of moment, and average coefficient of power, respectively. In these equations, Torque is denoted by T [Nm], density is denoted as ρ [kg/m^3], and A is the HDWT rotational area [m^2].

$$TSR = \frac{\omega R}{V_\infty} \tag{1}$$

$$C_m = \frac{T}{0.5\rho A R V_\infty^2} \tag{2}$$

$$C_p = \frac{T\omega}{0.5\rho A V_\infty^3} = \frac{T}{0.5\rho A R V_\infty^2} \times \frac{R\omega}{V_\infty} = C_m \times TSR \tag{3}$$

2.2. Geometry of the H-type Darrieus wind turbine and measurements of the cooling tower model

The HDWT parameters that is used and kept constant throughout this study is shown in Table 1 as these parameters produced desirable results in previous studies conducted by the authors [26]. A cooling tower will be added to be part of the computational domain. The cooling tower measurements for this study is as shown in Figure 1, which is taken from a study done by Liu et al [27] with its size reduced by a factor of 200.

Table 1. HDWT design

Parameter	Value
Airfoil profile	S-1046
Number of blades (***N***)	3
Diameter (***D***)	456 mm
Blade length (***H***)	200 mm
Chord length (c)	68.4 mm
Solidity ratio ($\boldsymbol{\sigma}$)	0.450

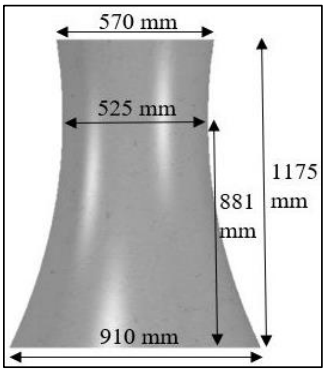

Figure 1. Cooling tower measurements.

2.3. Design and placement of the cycloidal diffuser

Table 2 and Figure 2 shows the dimensions of the cycloidal diffuser used for this study. The diffuser parameters selected are from previous studies done on flat-panel diffuser [21], [23], [24]. The diffusers' exit angle was kept at 35° because larger exit angles enhance the turbine the most as showed in earlier investigations by Watanabe et al. [23] and Dessoky et al. [24]. The inlet angle (shroud angle) was kept constant as 2° as previous studies have shown that the best angles are between 0° to 4° [24]. Flange of width 0.5D were also included in the design to cause a significant pressure to drop at the HDWT wake region to accelerate the air and draw higher velocity air through the diffuser, approaching the HDWT [23], [24]. Table 2 shows the parameters of the cycloidal diffuser adopted for this study where the shroud length will be tested at different lengths while other parts of the diffuser are kept constant. Figure 2 shows the cycloidal diffuser were positioned so that its throat is aligned with the middle part of the HDWT rotor.

Table 2. Cycloidal diffuser measurements.

Parameters	Dimensions
Shroud length (L_f)	0D, 0.25D (114 mm), 0.35D (159 mm), 0.48D (218 mm)
Diffuser length (L_b)	0.5D (228 mm)
Angle of inlet (γ)	2°
Angle of exit (ϕ)	35°
Width of throat (D_{dt})	486 mm
Clearance between HDWT and diffuser (c)	15 mm
Height (H_{df})	300 mm
Flange width (W)	0.5D (228 mm)

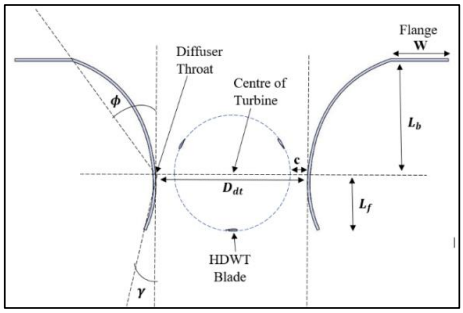

Figure 2. Two-dimensional view of cycloidal diffuser design.

2.4. Meshing and flow physics condition

Figure 3 depicts the meshed computational domain, which consists of a stationary region and a rotating region. A rectangular control volume and a cooling tower are combined to form the stationary domain. The cooling tower shape is included as a part of the stationary domain control volume with dimensions as described in section 2.2, whereas the cuboid shaped control volume measurements are set by using the ratio of the cooling tower outlet diameter. Solidworks is used to create the computational domain, cycloidal diffuser and HDWT, which is then loaded into Star CCM+ for 3-dimensional numerical analysis. The HDWT is positioned in the rotating zone, $0.5D$ above the cooling tower outlet, with D being the HDWT's diameter. An interface is created surrounding the HDWT to separate the rotating and stationary region and sliding mesh is employed for the interface. The blades of the HDWT were set to be no-slip wall boundary. Velocity inlet of 3.7 m/s was set at the bottom of cooling tower, which is accelerated by the cooling tower shape, reaching desired 9 m/s wind speed at the outlet. The type of mesh employed for this study is a three-dimensional polyhedral mesh for the whole computational domain. Finer mesh was used around the HDWT rotating domain and the HDWT blades surface and mesh refinement was done for the HDWT wake region. Prism layer was produced around the HDWT blades using growth size rate of 1.2, first prism layer thickness of 3×10^{-5} m and total thickness set as 1% of the HDWT diameter to obtain value lower than 1 for the near wall y^+. For flow physics, three-dimensional implicit unsteady Reynolds-Averaged Navier-Stokes (URANS) equations were employed with Menter k-ω shear stress transport (SST) turbulence model and 2nd order temporal discretization. The dynamic viscosity and air density was set constant at 1.85508×10^{-5} Pa.s and 1.18415 kg/m^3, respectively. To obtain the desired TSR ranges of 1.5 to 3.0 for this study, the rotational speed of the HDWT was inputted as 59.21 rad/s to 118.42 rad/s Lastly, to achieve converged solution, 20 inner iterations were used.

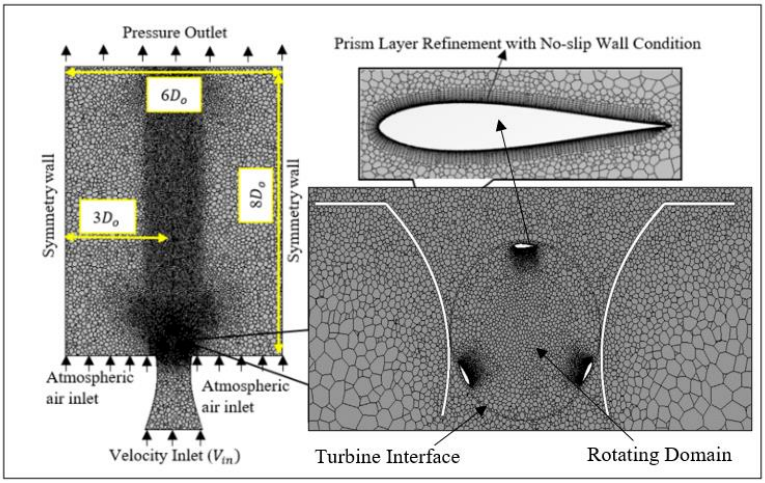

Figure 3. Meshed computational domain with cycloidal diffuser.

3. Validation of the computational model

Grid independence test and time step sensitivity study were carried out for accuracy of result. The C_m value of HDWT were measured once it converges after 7 rotations. From Figure 4, 5.6 million cells were chosen as it produces C_m variation below 1% after further refinement of mesh. The size of the time steps was chosen to spin the HDWT by 1°, 2.5°, 5° and 10° degrees to measure a single blade C_m against azimuthal angle. Figure 5 shows that bigger time step deviates the peak blade C_m towards higher azimuthal angle and overpredicts the C_m values from 170° to 280°. Final time step chosen was 2.5° which takes about 72 hours of computational time to reach quasi-static convergence to balance computational cost as the 1° takes about 180 hours to reach quasi-static convergence.

Then, the grid size and time step chosen was validated against Castelli et al. [28] experimental study and Rezaeiha et al. [29] two-dimensional numerical study by extending the computational domain to a full rectangular domain. Table 3 shows the validation parameters. Results in Figure 6 confirms the suitability of the current mesh to be used to conduct this numerical study as it demonstrates acceptable agreement to past literature compared.

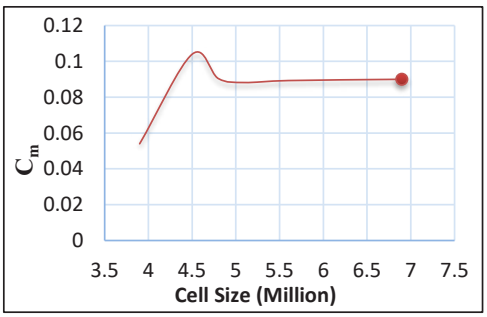

Figure 4. Grid independence study graph.

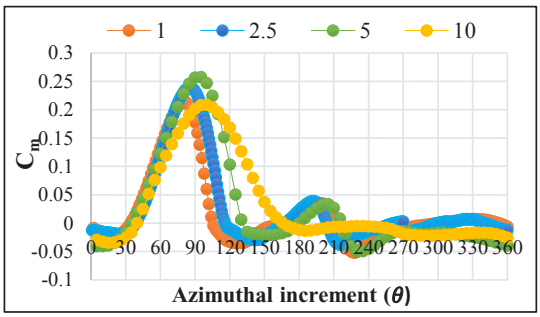

Figure 5. Time step study graph.

Table 3. Simulation validation condition.

Setup	Values
Airfoil type	NACA 0021
Inlet wind velocity (V_{in})	9.00 m/s
HDWT diameter (D)	1.030 m
HDWT height (H)	1.456 m
Solidity ratio (σ)	0.25
Tip speed ratios (TSR)	1.44 - 3.30

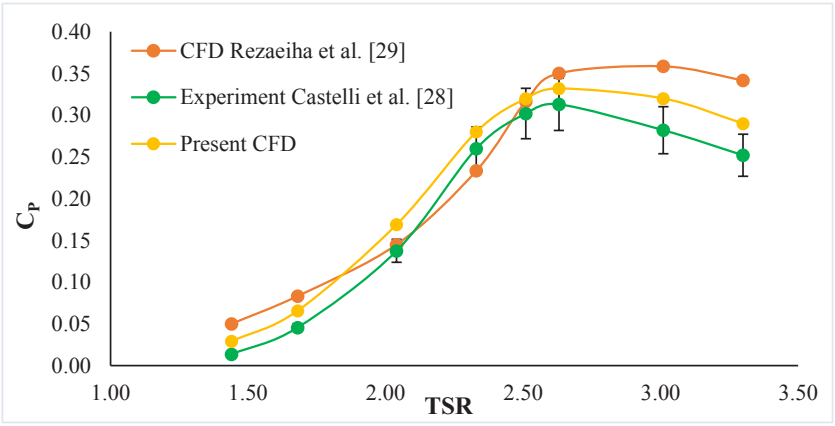

Figure 6. Validation of the computational set-up for this study.

4. Results and Discussion

This computational study was conducted by first measuring the power coefficient values of the HDWT without the diffuser under the cooling tower exhaust air at TSR 1.5 to TSR 3.0. Then, cycloidal diffuser with different shroud lengths were added to the design and the augmented HDWT performance were measured at the same TSRs as the bare HDWT. The coefficient of moment coefficient and coefficient of power of the bare HDWT and augmented HDWT are provided in subsection 4.1. The flow analysis around HDWT with different diffuser shroud lengths are provided in subsection 4.2. In subsection 4.3, the comparison between the flow characteristics of the HDWT without diffuser and HDWT with best cycloidal diffuser shroud length of $0.48D$ are provided and discussed.

4.1. Coefficient of moment and power of the tested exhaust air energy extractor designs.

The values of the coefficient of moment and coefficient of power of the bare HDWT model and HDWT with cycloidal diffuser with different shroud length are provided in Figure 7 and 8, respectively. From the figure, it is observed that the maximum C_p achieved by the augmented HDWT is 0.4048 with using diffusers of shroud length $0.48D$ at TSR 2.0, which is a 26.66% improvement compared to the case of HDWT without any diffuser. The cycloidal diffuser with shroud length of $0.48D$ increases the HDWT performance at all TSRs and the cycloidal diffuser with shroud length of $0.35D$ increases the HDWT performance at TSRs of 1.5 and 2.0. However, the other cycloidal diffusers did not augment the HDWT power coefficient. The single blade instantaneous coefficient of moment comparison for one complete rotation after the simulation converges between the bare HDWT and HDWT with the best shrouded cycloidal diffuser design at TSR 2.0 is shown in Figure 9. The shrouded diffuser design produced more positive moment coefficient throughout a single rotation which results in the averaged power coefficient being higher than the bare HDWT design. The HDWT augmented by the cycloidal diffuser produces biggest difference in instantaneous moment coefficient at azimutal angles from 0° to 40° and from 120° to 170°.

4.2. Analysis of the flow around HDWT with cycloidal diffuser of different shroud length at TSR 2.0.

The velocity contour in Figure 9 explains the difference in performance for the different shroud length. From figure 9 (a), there are no shroud included ($0D$) which means the exhaust air is not guided at the windward side of the HDWT. When compared to cycloidal diffuser with shroud as indicated in Figures 9 (b) and (c), the exhaust air is being guided and accelerated before interacting with the HDWT blade. The longer shroud length ($0.48D$) shows better flow characteristics as the wind velocity near the blade surface has higher speed which in turn reduces the pressure, creating bigger pressure difference between the top and bottom side of blade, resulting in higher lift generated.

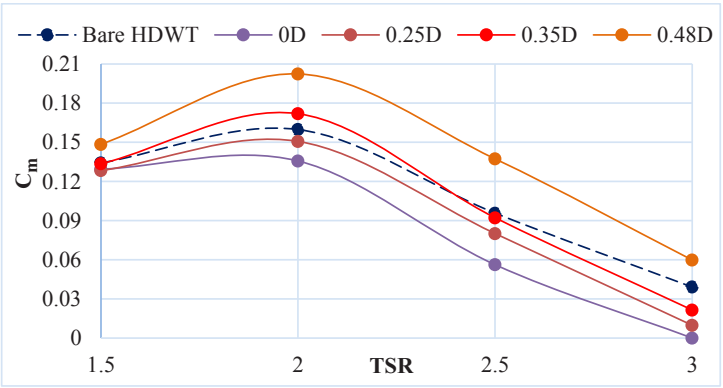

Figure 7. Coefficient of moment graph.

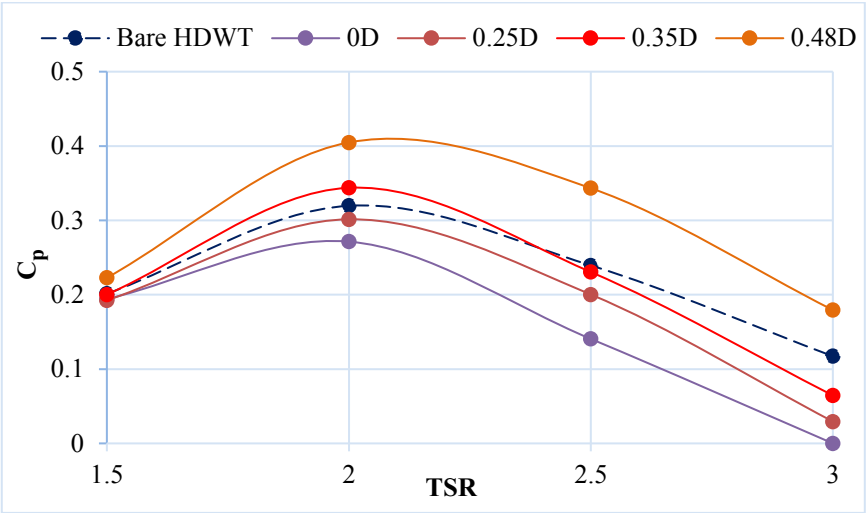

Figure 8. Coefficient of power graph.

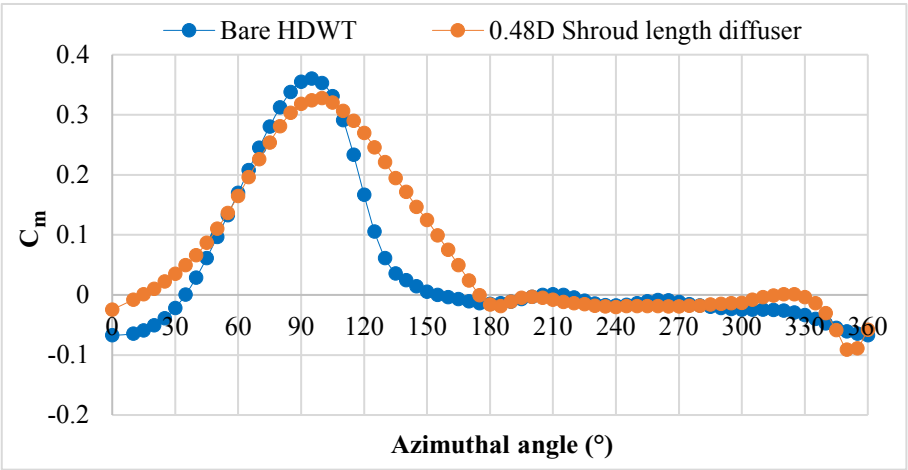

Figure 9. Single blade instantaneous C_m for one complete rotation of the bare HDWT case and the HDWT with cycloidal diffuser of shroud length $0.48D$ at TSR 2.0.

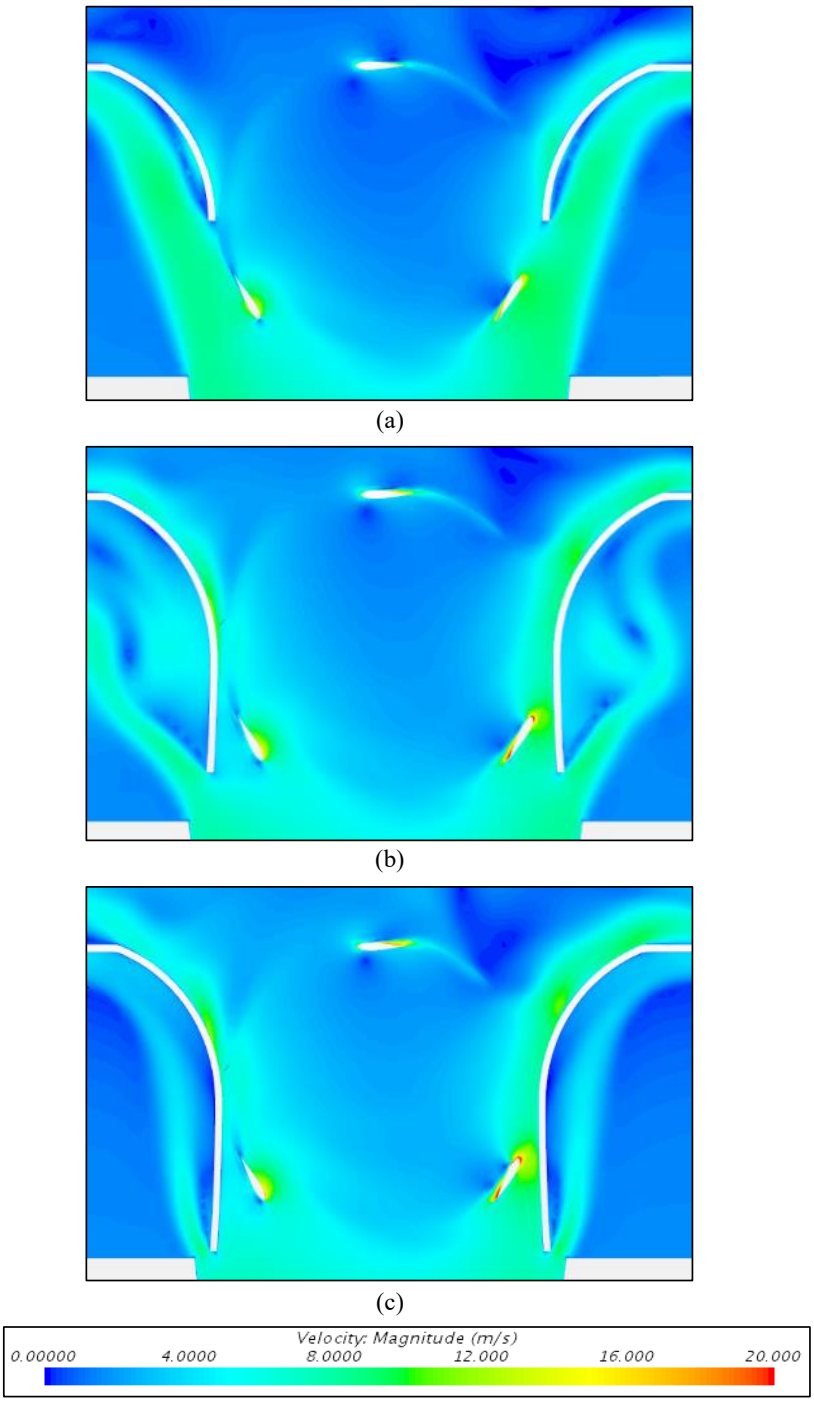

Figure 10. Velocity contour around HDWT with cycloidal diffusers with shroud length of: (a) 0D, (b) 0.35D and (c) 0.48D at TSR 2.0.

4.3. Comparison between the flow characteristics of bare HDWT and HDWT enclosed by cycloidal diffuser of shroud length 0.48D at TSR 2.0.

The velocity and pressure contours to compare the HDWT without any diffuser and HDWT enclosed by the cycloidal diffuser of shroud length 0.48*D* at TSR 2.0 are provided in Figure 11 and 12, respectively. The HDWT in both figures are at azimuthal angle, (θ) of (a) 0° and (b) 30° with blade 1 as reference to the x-axis. It can be seen from Figure 11 that the air flow near the cycloidal diffuser wall has higher velocity, at the windward and leeward side of the HDWT compared to the bare HDWT case. The increase in the exhaust air velocity caused by the diffuser creates high pressure difference between the upwind and downwind region of the HDWT as seen in Figure 12. This causes the HDWT blades at upwind region, near the diffuser wall to have much higher instantaneous moment coefficient than that of bare HDWT as seen in Figure 9 (0° to 60°) and (120° to 180°) as the blades experiences higher pressure difference between the pressure side and suction side of the blades, increasing its lift coefficient. Figure 11 (b) shows that at θ=30°, the air velocity around blade 1 (30°) and blade 2 (150°) of the diffuser augmented HDWT are higher than the bare HDWT which creates higher pressure difference between the blades top and bottom surface as seen in Figure 12 (b). The pressure difference around blade 1 (0°) and blade 2 (120°) of the diffuser augmented HDWT is also slightly higher than the bare HDWT blades at azimuthal rotation of 0° as seen in Figure 12 (a). Overall, these big increase of instantaneous moment coefficients at the stated blade angles contributed to the increase in average moment and power coefficients of the diffuser augmented HDWT, resulting it to perform better than the bare HDWT.

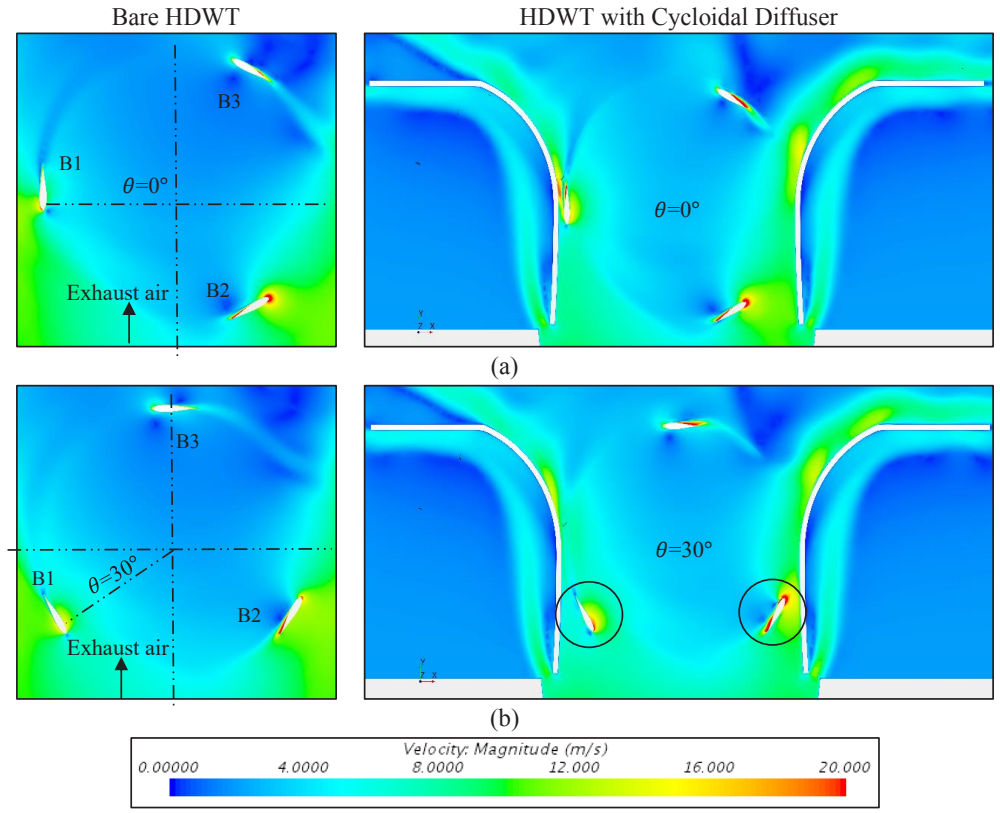

Figure 11. Velocity contour of bare HDWT case (left) and HDWT with shrouded cycloidal diffuser case (right) at TSR of 2.0 at azimuthal location of; (a) θ=0°, (b) θ=30°.

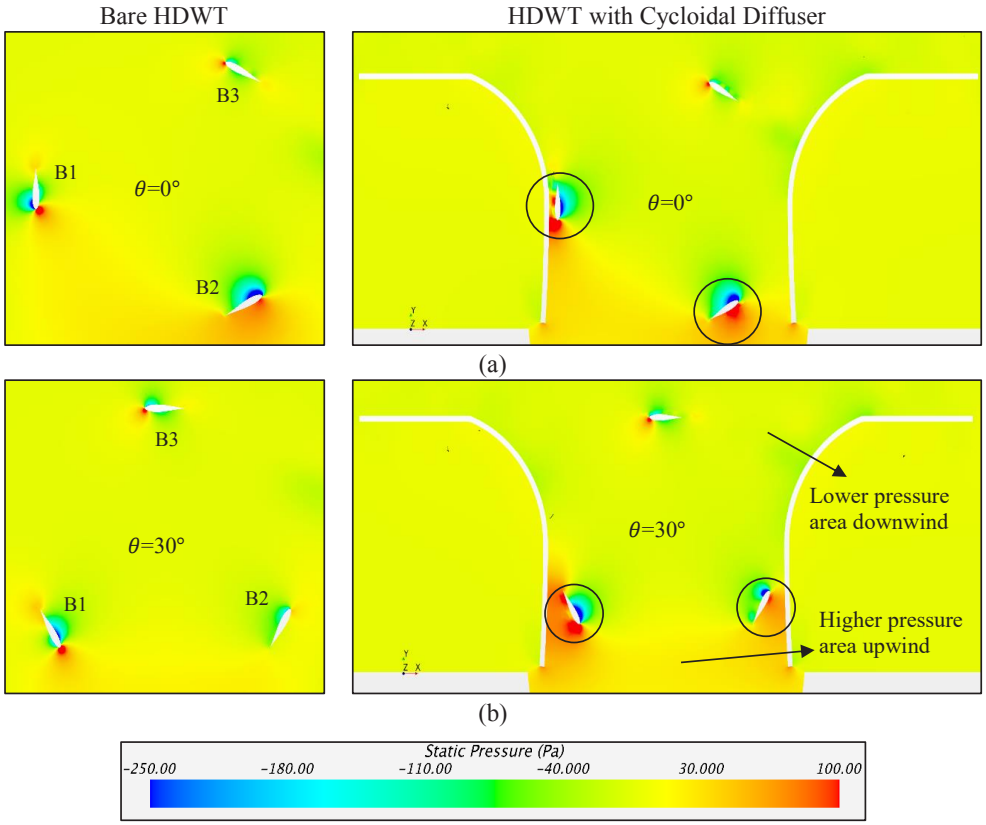

Figure 12. Pressure contour of bare HDWT case (left) and HDWT with shrouded cycloidal diffuser case (right) at TSR of 2.0 at azimuthal location of; (a) θ=0°, (b) θ=30°.

5. Conclusion

The present study focuses on improving the cycloidal diffuser design to enhance the performance of the HDWT for cooling tower exhaust air energy extraction. Three-dimensional computational simulation study was conducted giving maximum C_p of 0.4048 at TSR 2.0 when the shroud length of the cycloidal diffuser is set at $0.48D$ (218 mm). Flow analysis has also been done which shows the flow around the HDWT is enhanced greatly when the shroud length extends up to the cooling tower exhaust air outlet.

Acknowledgement

The authors express gratitude to Curtin University Malaysia for making the facilities available, distinctly the software licensing of Star CCM+ to conduct the numerical analysis for this study. The authors would also like to extend their heartfelt appreciation to the Ministry of Higher Education (MOHE) Malaysia for providing the financial support through the Fundamental Research Grant Scheme (FRGS Grant: FRGS/1/2018/TK10/CURTIN/03/1) to complete this research.

References

[1] B. Looney, "Statistical Review of World Energy globally consistent data on world energy markets . and authoritative publications in the field of energy," *Rev. World Energy data*, vol. 70, pp. 8–20, 2021.

[2] International Energy Agency, "Global Energy Review 2021," *Glob. Energy Rev. 2020*, pp. 1–36, 2021, [Online]. Available: https://iea.blob.core.windows.net/assets/d0031107-401d-4a2f-a48b-9eed19457335/GlobalEnergyReview2021.pdf.

[3] J. Lee and F. Zhao, "Gobal Wind Report 2021," *Glob. Wind Energy Counc.*, p. 75, 2021, [Online]. Available: http://www.gwec.net/global-figures/wind-energy-global-status/.

[4] R. Kumar, K. Raahemifar, and A. S. Fung, "A critical review of vertical axis wind turbines for urban applications," *Renew. Sustain. Energy Rev.*, vol. 89, no. April, pp. 281–291, 2018, doi: 10.1016/j.rser.2018.03.033.

[5] I. Hashem and M. H. Mohamed, "Aerodynamic performance enhancements of H-rotor Darrieus wind turbine," *Energy*, vol. 142, pp. 531–545, 2018, doi: 10.1016/j.energy.2017.10.036.

[6] B. Hand, G. Kelly, and A. Cashman, "Aerodynamic design and performance parameters of a lift-type vertical axis wind turbine: A comprehensive review," *Renew. Sustain. Energy Rev.*, vol. 139, no. December 2019, p. 110699, 2021, doi: 10.1016/j.rser.2020.110699.

[7] A. Rezaeiha, H. Montazeri, and B. Blocken, "Towards optimal aerodynamic design of vertical axis wind turbines: Impact of solidity and number of blades," *Energy*, vol. 165, pp. 1129–1148, 2018, doi: 10.1016/j.energy.2018.09.192.

[8] A. Sagharichi, M. Zamani, and A. Ghasemi, "Effect of solidity on the performance of variable-pitch vertical axis wind turbine," *Energy*, vol. 161, pp. 753–775, 2018, doi: 10.1016/j.energy.2018.07.160.

[9] Y. Celik, L. Ma, D. Ingham, and M. Pourkashanian, "Journal of Wind Engineering & Industrial Aerodynamics Aerodynamic investigation of the start-up process of H-type vertical axis wind turbines using CFD," *J. Wind Eng. Ind. Aerodyn.*, vol. 204, no. November 2019, p. 104252, 2020, doi: 10.1016/j.jweia.2020.104252.

[10] Z. Zhao, D. Wang, T. Wang, W. Shen, H. Liu, and M. Chen, "Review article A review : Approaches for aerodynamic performance improvement of lift-type vertical axis wind turbine," *Sustain. Energy Technol. Assessments*, vol. 49, no. November 2021, p. 101789, 2022, doi: 10.1016/j.seta.2021.101789.

[11] K. H. Wong, W. T. Chong, N. L. Sukiman, S. C. Poh, Y. C. Shiah, and C. T. Wang, "Performance enhancements on vertical axis wind turbines using flow augmentation systems: A review," *Renew. Sustain. Energy Rev.*, vol. 73, no. January, pp. 904–921, 2017, doi: 10.1016/j.rser.2017.01.160.

[12] Hensley John C., *Cooling Tower Fundamentals*, 2nd ed. Overland Park, Kansas USA: SPX Cooling Technologies, Inc, 2009.

[13] W. T. Chong *et al.*, "The experimental study on the wind turbine's guide-vanes and diffuser of an exhaust air energy recovery system integrated with the cooling tower," *Energy Convers. Manag.*, vol. 87, pp. 145–155, 2014, doi: 10.1016/j.enconman.2014.07.009.

[14] S. Tabatabaeikia *et al.*, "Computational and experimental optimization of the exhaust air energy recovery wind turbine generator," *Energy Convers. Manag.*, vol. 126, pp. 862–874, 2016, doi: 10.1016/j.enconman.2016.08.039.

[15] H. Berhanu, D. Gudeta, A. Haiter Lenin, and B. Karthikeyan, "Numerical and experimental investigation of an exhaust air energy recovery Savonius wind turbine for power production," *Mater. Today Proc.*, no. xxxx, 2021, doi: 10.1016/j.matpr.2021.02.675.

[16] A. A. Nimje and N. M. Gandhi, "Design and development of small wind turbine for power generation through high velocity exhaust air," *Renew. Energy*, vol. 145, pp. 1487–1493, 2020, doi: 10.1016/j.renene.2019.06.065.

[17] M. Eshagh Nimvari, H. Fatahian, and E. Fatahian, "Performance improvement of a Savonius

vertical axis wind turbine using a porous deflector," *Energy Convers. Manag.*, vol. 220, no. March, p. 113062, 2020, doi: 10.1016/j.enconman.2020.113062.

[18] E. Fatahian, F. Ismail, M. Hafifi Hafiz Ishak, and W. Shyang Chang, "An innovative deflector system for drag-type Savonius turbine using a rotating cylinder for performance improvement," *Energy Convers. Manag.*, vol. 257, no. March, p. 115453, 2022, doi: 10.1016/j.enconman.2022.115453.

[19] K. Qasemi and L. N. Azadani, "Optimization of the power output of a vertical axis wind turbine augmented with a flat plate deflector," *Energy*, vol. 202, p. 117745, 2020, doi: 10.1016/j.energy.2020.117745.

[20] W. H. Chen *et al.*, "Optimization of a vertical axis wind turbine with a deflector under unsteady wind conditions via Taguchi and neural network applications," *Energy Convers. Manag.*, vol. 254, no. January, p. 115209, 2022, doi: 10.1016/j.enconman.2022.115209.

[21] A. Dilimulati, T. Stathopoulos, and M. Paraschivoiu, "Wind turbine designs for urban applications: A case study of shrouded diffuser casing for turbines," *J. Wind Eng. Ind. Aerodyn.*, vol. 175, no. November 2017, pp. 179–192, 2018, doi: 10.1016/j.jweia.2018.01.003.

[22] X. H. Wang, K. H. Wong, W. T. Chong, J. H. Ng, X. B. Xiang, and C. T. Wang, "Experimental investigation of a diffuser-integrated vertical axis wind turbine," *IOP Conf. Ser. Earth Environ. Sci.*, vol. 463, no. 1, 2020, doi: 10.1088/1755-1315/463/1/012153.

[23] K. Watanabe, S. Takahashi, and Y. Ohya, "Application of a diffuser structure to vertical-axis wind turbines," *Energies*, vol. 9, no. 6, 2016, doi: 10.3390/en9060406.

[24] A. Dessoky, G. Bangga, T. Lutz, and E. Krämer, "Aerodynamic and aeroacoustic performance assessment of H-rotor darrieus VAWT equipped with wind-lens technology," *Energy*, vol. 175, pp. 76–97, 2019, doi: 10.1016/j.energy.2019.03.066.

[25] E. Singh, S. Roy, Y. Ke San, M. C. Law, and P. Kumar, *Computational Analysis of Air Energy Extractors for Guided Flow Exhaust Applications*, vol. 301. Springer Nature Singapore, 2023.

[26] E. Singh, S. Roy, Y. K. San, and L. M. Chiat, "Optimisation of H-Darrieus VAWT Solidity for Energy Extraction in Cooling Tower Exhaust Systems," *J. Adv. Res. Fluid Mech. Therm. Sci.*, vol. 91, no. 2, pp. 51–61, 2022, doi: 10.37934/arfmts.91.2.5161.

[27] Z. Liu, C. Zhang, and T. Ishihara, "Numerical study of the wind loads on a cooling tower by a stationary tornado-like vortex through LES," *J. Fluids Struct.*, vol. 81, pp. 656–672, 2018, doi: 10.1016/j.jfluidstructs.2018.06.001.

[28] M. Raciti Castelli, A. Englaro, and E. Benini, "The Darrieus wind turbine: Proposal for a new performance prediction model based on CFD," *Energy*, vol. 36, no. 8, pp. 4919–4934, 2011, doi: 10.1016/j.energy.2011.05.036.

[29] A. Rezaeiha, I. Kalkman, and B. Blocken, "Effect of pitch angle on power performance and aerodynamics of a vertical axis wind turbine," *Appl. Energy*, vol. 197, pp. 132–150, 2017, doi: 10.1016/j.apenergy.2017.03.128.